eLIFE elifesciences.org

RESEARCH ARTICLE

Figures and figure supplements

Wiz binds active promoters and CTCF-binding sites and is required for normal behaviour in the mouse

Luke Isbel *et al*

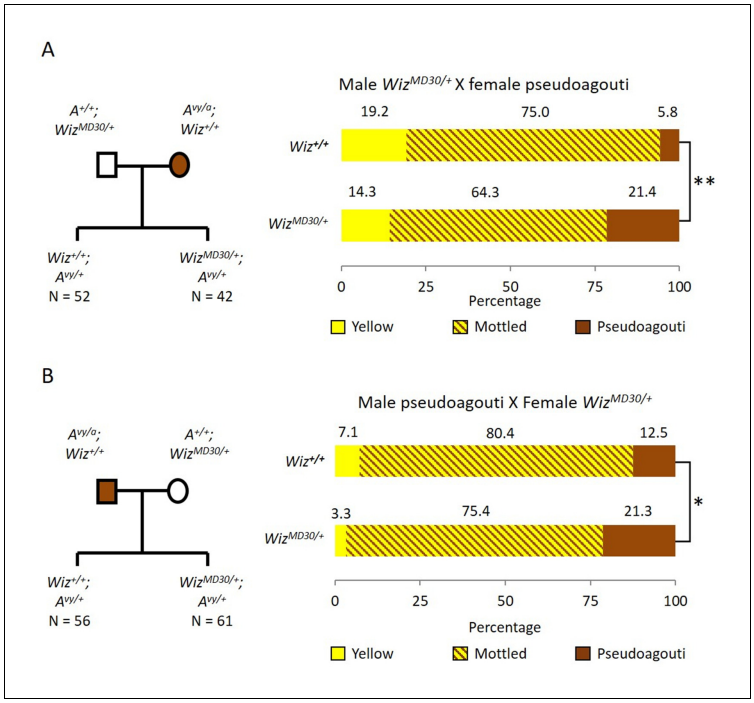

Figure 1. Wiz haploinsufficiency increases silencing at the A^{vy} locus. Pedigree charts (left) are shown for generating F1 mice heterozygous for the A^{vy} allele and either wildtype or heterozygous for $Wiz^{MommeD30}$. $Wiz^{MommeD30/+}$ mice were crossed to pseudoagouti A^{vy}/a mice, numbers of F1 mice in each cohort are indicated. The proportions of coat colours for F1 mice are shown (right) from a cross with either a $Wiz^{MommeD30/+}$ sire (**A**) or dam (**B**). Chi-squared tests were carried out to determine significance, *p-value<0.05, **p-value<0.005.
DOI: 10.7554/eLife.15082.002

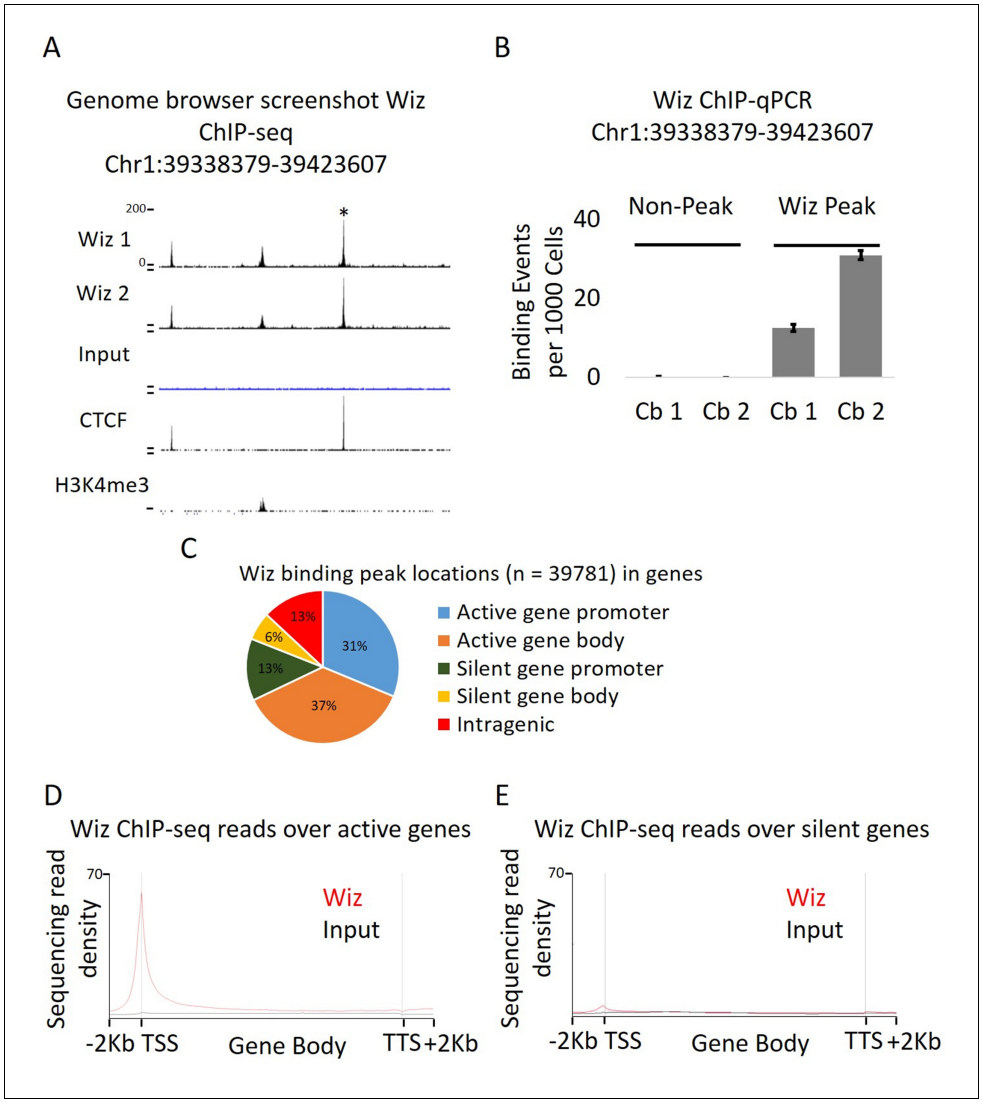

Figure 2. Wiz binds across the genome and at promoter elements. (**A**) ChIP-seq was performed for Wiz in the adult male cerebellum, a screenshot is shown of a random Wiz-enriched site (* indicated) with the two ChIP-seq replicates and input, from the ~40,000 significantly enriched peaks. Encode data for CTCF and H3K4me3 is also included. (**B**) Enrichment for Wiz in two cerebellum samples (Cb1 and Cb2) is shown by ChIP-qPCR, with primers located in regions not enriched for Wiz in ChIP-seq data and primers flanking the * indicated ChIP-seq peak from (**A**). Enrichment is represented as binding events detected per 1000 cells and are generated by running samples in parallel with known amounts of genomic DNA. Error bars indicate S.D. from 3 technical replicates. (**C**) The percentage is shown of Wiz peaks that overlap with the promoter (up to 2 kb from a TSS) and genic sequence of genes that were classified as active or silenced, according to RNA-seq data mapped to Ensembl genes annotations. (**D**) Wiz ChIP-seq (and Input) occupancy over all Ensembl gene bodies is shown as deep sequencing read density along the transcription unit, including 2 kb up and downstream of the transcriptional start and stop site. Genes were separated into either active or silenced transcriptional states, as in **C**.

DOI: 10.7554/eLife.15082.003

The following source data is available for figure 2:

Source data 1. Anti-Wiz antibody co-immunoprecipitation.

DOI: 10.7554/eLife.15082.004

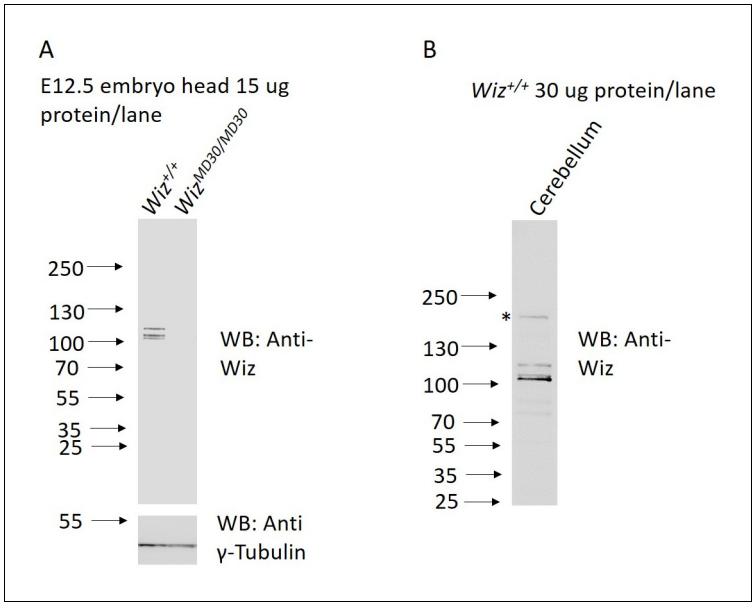

Figure 2—figure supplement 1. Anti-Wiz antibody western blotting. (**A**) Western blotting for Wiz using an NBP180586 anti-Wiz antibody is shown for total protein lysates from E12.5 *Wiz*$^{+/+}$ and *Wiz*$^{MommeD30/MommeD30}$ embryo head. Three bands at ~100 kD represent Wiz isoforms, consistent with UCSC gene splice variants, in *Wiz*$^{+/+}$ sample and are absent in *Wiz*$^{MommeD30/\ MommeD30}$ sample. Western blotting with an anti-γ-Tubulin antibody is shown as a loading control. (**B**) Anti-Wiz antibody staining in adult cerebellum, showing the short (~100–120 KDa) isoforms present in embryo head protein extract, as well as a long (~160 KDa) isoform previously reported to be expressed (***Matsumoto et al., 1998***).

DOI: 10.7554/eLife.15082.005

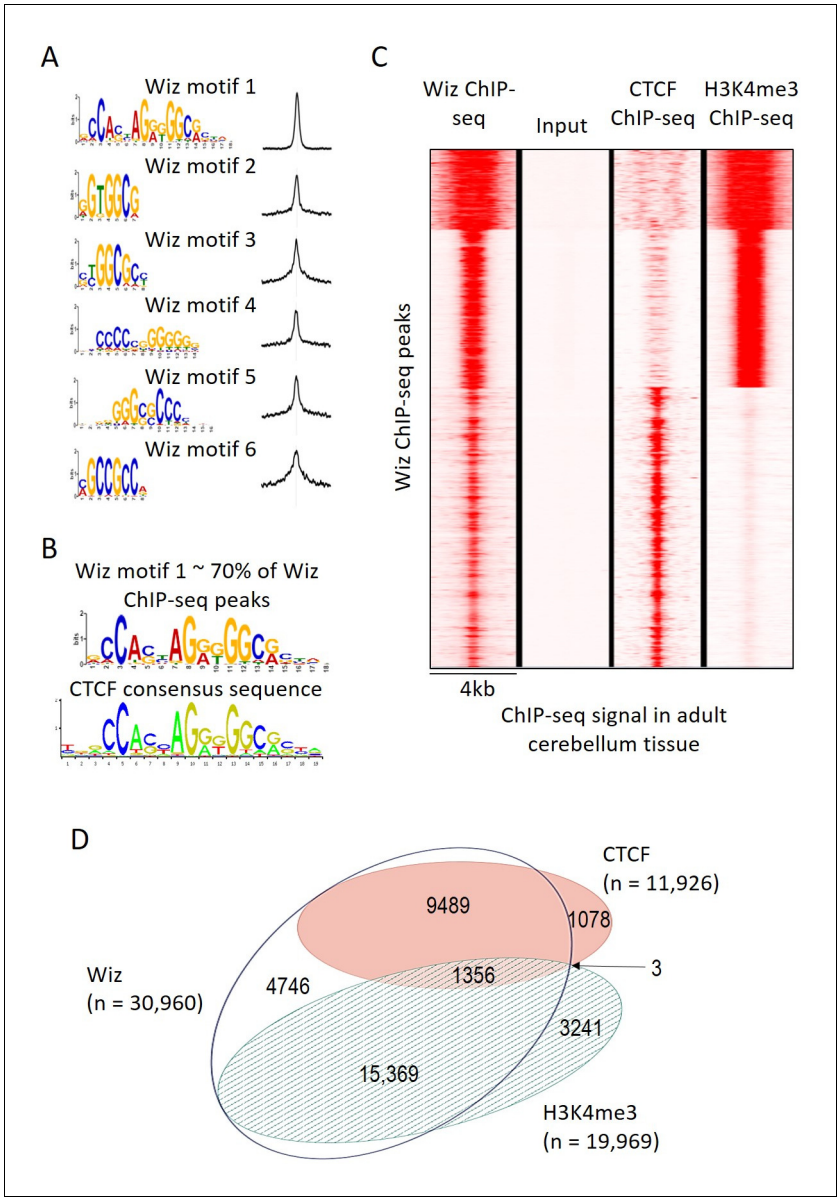

Figure 3. Wiz binding consensus shows a high degree of overlap with that for CTCF. (**A**) The six most enriched motifs in Wiz ChIP-seq peaks (n = 39,781) and their distribution inside peaks are shown. (**B**) The most significant of these matches the CTCF-binding site consensus sequence (JASPAR CORE database - MA0139.1). (**C**) Read density for Wiz and the Encode CTCF and H3K4me3 ChIP-seq datasets were calculated across a 4 kb region centred on the ~40,000 Wiz ChIP-seq peaks. Input sequencing from the Wiz ChIP-seq experiment is also shown. Loci are clustered by the similarity of read density and datasets were normalized to the smallest sized library. (**D**) Venn diagram showing the overlap for Wiz, CTCF and H3K4me3 ChIP-seq peaks. An overlap was defined as at least one base of sequence occupied by a significantly enriched peak ($p \leq 1 \times 10^{-20}$) from two datasets.
DOI: 10.7554/eLife.15082.006

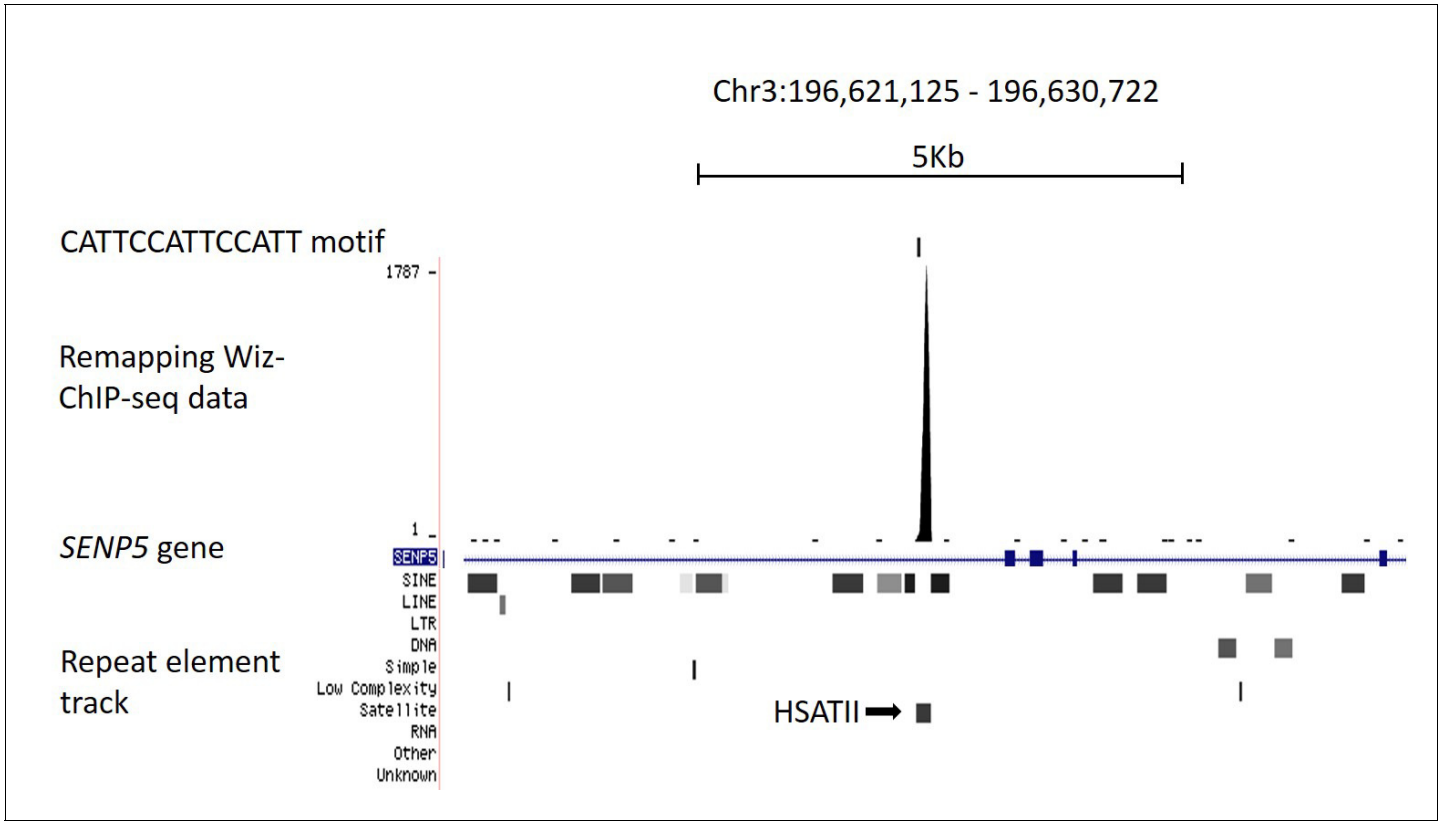

Figure 3—figure supplement 1. Remapping publically available Wiz ChIP-seq data. (B) Shown is a UCSC genome browser screenshot of the *SENP5* gene focussing on the consensus binding site (CATTCCATTCCATT motif) reported in ***Bian et al. (2015)***. The consensus binding site is indicated. Strong enrichment is seen for the Wiz ChIP-seq data, shown as a continuous read-depth score, at the CATTCCATTCCATT motif, though this occurs over a HSATII satellite element (shown in the repeat masker track) and is likely to be a mapping artefact.
DOI: 10.7554/eLife.15082.007

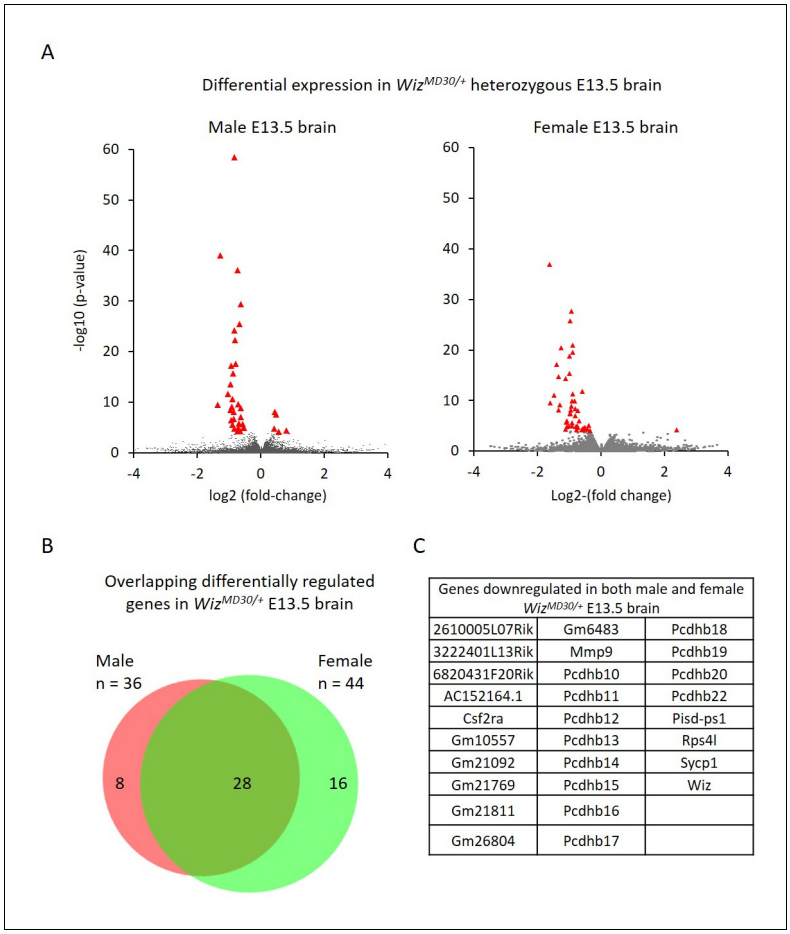

Figure 4. Differential gene expression in male and female $Wiz^{MommeD30/+}$ E13.5 brains. (**A**) Volcano plots show the log2 fold-change (x-axis) in the average expression of genes in $Wiz^{MommeD30/+}$ E13.5 brains compared to $Wiz^{+/+}$ E13.5 brains. Shown is data for males (left, n = 3 per genotype) and females (right, n = 2 per genotype). Significance is shown on a –log10 scale, those genes indicated in red are significantly differentially regulated with an adjusted p-value<0.05. (**B**) The overlap in differentially expressed genes is shown for the male and female embryonic brains, the majority of transcripts differentially expressed represent a common set between the sexes, listed in alphabetical order in (**C**), and all of these decrease in expression.

DOI: 10.7554/eLife.15082.008

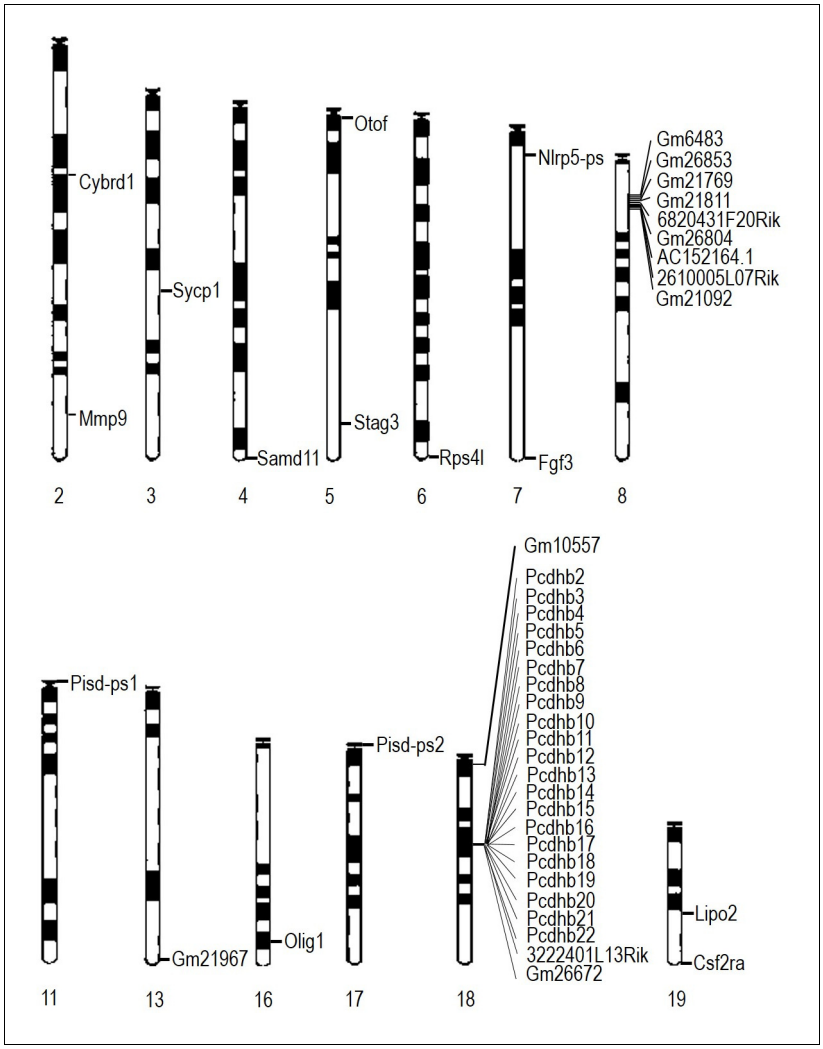

Figure 4—figure supplement 1. Location of differentially expressed genes in E13.5 *Wiz*$^{MommeD30/+}$ brains. The locations of down regulated genes differentially expressed in E13.5 brains of *Wiz*$^{MommeD30/+}$ mice (combined from male and female datasets) are shown on mouse chromosomes. The *Wiz* gene is not shown.
DOI: 10.7554/eLife.15082.009

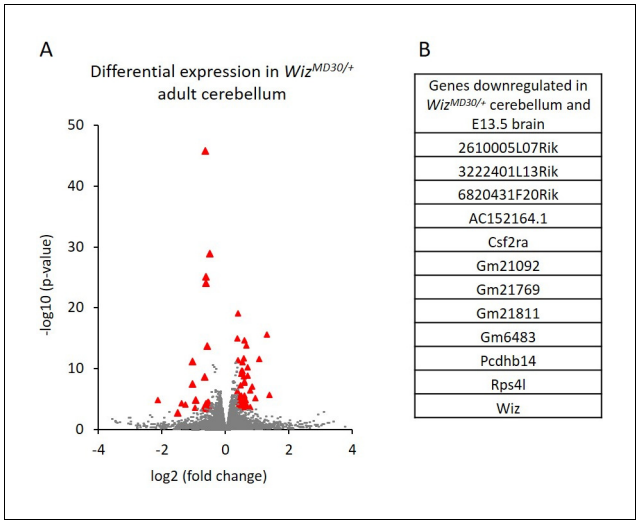

Figure 5. Differential gene expression in $Wiz^{MommeD30/+}$ adult cerebellum. (**A**) The log2 fold-change (x-axis) in the average expression of genes is shown for $Wiz^{MommeD30/+}$ and $Wiz^{+/+}$ cerebellum. Three male biological replicates were used per genotype. Significance is shown on a –log10 scale, those genes indicated in red are significantly differentially regulated. (**B**) A list of significantly differentially regulated genes in $Wiz^{MommeD30/+}$ cerebellum that were also deregulated in E13.5 $Wiz^{MommeD30/+}$ brains.

DOI: 10.7554/eLife.15082.010

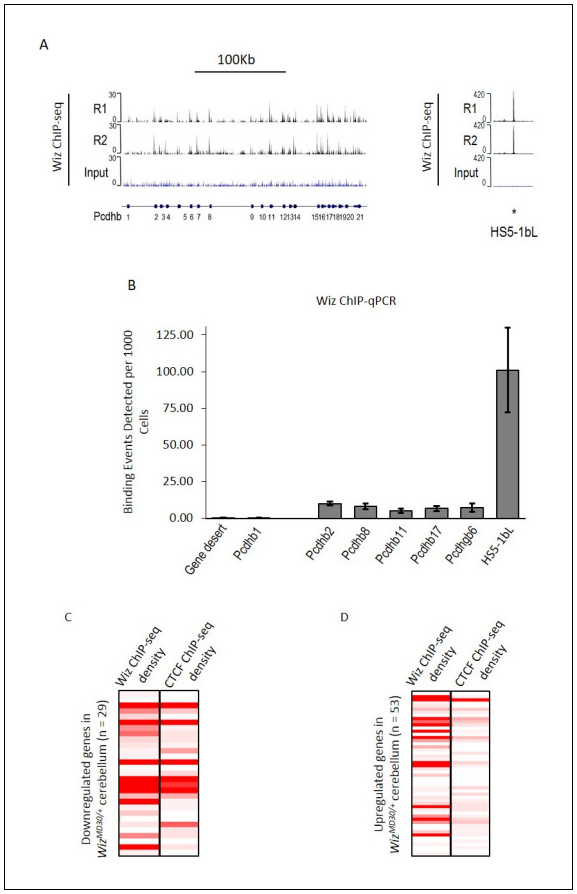

Figure 6. Wiz binding at the protocadherin β locus in the adult cerebellum. (**A**) Genome browser screenshots of the protocadherin β locus and the HS5-1bL enhancer (*indicated) located ~400 Kb downstream. Shown are Wiz ChIP-seq data generated in the adult cerebellum as the read depth along the locus. Wiz binds promoters of the Pcdhb locus (left) and is enriched more at the downstream HS5-1bL enhancer (right), the relative binding of Wiz is indicated by the altered scale bar. The location of the Pcdhb genes, are indicated. (**B**) ChIP-qPCR was performed using the anti-Wiz antibody for two negative Wiz-enrichment sites, with primers located in a gene desert and at *Pcdhb1*, which was not enriched in ChIP-seq, and six positive Wiz-enrichment sites, including the promoters of four Pcdhb genes, the promoter of a Pcdhg gene and the downstream HS5-1bL enhancer. Enrichment is represented as binding events detected per 1000 cells and are generated by running samples in parallel with known amounts of genomic DNA. Error bars are the SEM from 3 biological replicates. (**C**) Shown is Wiz ChIP-seq read density in adult cerebellum as a heatplot for the 29 genes that decreased and (**D**) the 53 genes that increased, in expression in the cerebellum of $Wiz^{MommeD30/+}$ mice. Also shown is CTCF ChIP-seq read density. ChIP-seq density was calculated for the 1 Kb surrounding the TSS of each gene and genes are ranked from the lowest to the highest fold change in

Figure 6 continued on next page

Figure 6 continued

each case. Datasets were normalized to the size of smallest library.

DOI: 10.7554/eLife.15082.011

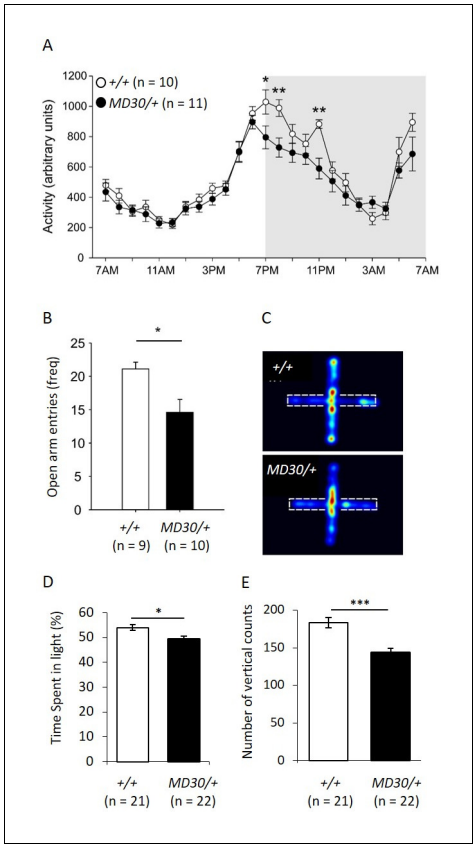

Figure 7. *Wiz*$^{MommeD30/+}$ mice show decreased activity and increased anxiety-like behaviour. (**A**) Line graph illustrating the average 24 hr activity profile from *Wiz*$^{+/+}$ and *Wiz*$^{MommeD30/+}$ mice, collapsed from 12 days of testing. The pattern of activity is broadly similar between the genotypes, though *Wiz*$^{MommeD30/+}$ mice show decreased activity in the first two hours and the fifth hour of the active phase of the light/dark cycle. Grey box indicates the dark phase of the light/dark cycle. (**B**) Bar graph showing decreased open arm entries among *Wiz*$^{MommeD30/+}$ mice compared with *Wiz*$^{+/+}$ mice, after 5 min intervals on the EPM test. (**C**) Heat map of locomotor activity on the EPM from a representative *Wiz*$^{+/+}$ mouse (top) and a representative *Wiz*$^{MommeD30/+}$ mouse (bottom). Broken lines indicate the location of the closed arms of the EPM. (**D**) Percentage of time *Wiz*$^{+/+}$ (n = 21) and *Wiz*$^{MommeD30/+}$ (n = 22) mice spent in the light portion of a light-dark test. (**E**) The number of vertical counts (rearing) *Wiz*$^{+/+}$ and *Wiz*$^{MommeD30/+}$ mice showed in the light-dark test. Error bars represent ± SEM, *p-value <0.05, **p-value 0.005, ***p-value <0.0005.

DOI: 10.7554/eLife.15082.012

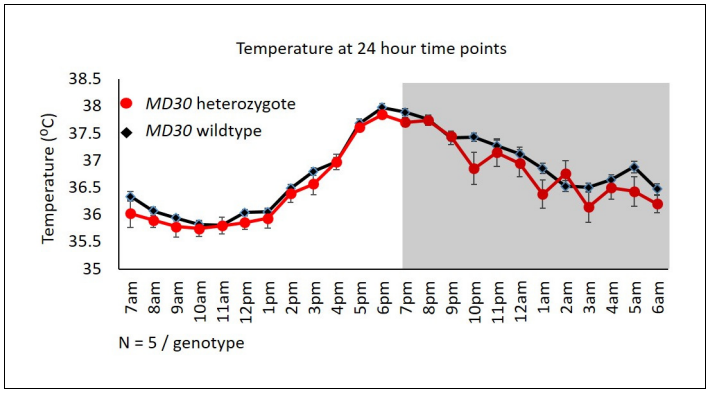

Figure 7—figure supplement 1. No difference in temperature in $Wiz^{MommeD30/+}$ mice. Telemetry data from across 3 days were collapsed into hourly intervals and the average temperature of $Wiz^{+/+}$ (black data points) and $Wiz^{MommeD30/+}$ (red data points) mice is shown. Lights on is indicated by light background and lights off is indicated by grey background. Numbers of mice for each cohort are indicated. Error bars are the SEM.
DOI: 10.7554/eLife.15082.013